Available online at www.sciencedirect.com
SCIENCE DIRECT®
Biochemical Pharmacology 67 (2004) 1677–1688
Biochemical Pharmacology
www.elsevier.com/locate/biochempharm

Role of zinc and iron chelation in apoptosis mediated by tachpyridine, an anti-cancer iron chelator

Rong Zhao[a,b], Roy P. Planalp[c], Rong Ma[b,d], Bryan T. Greene[a,b], Bradley T. Jones[e], Martin W. Brechbiel[f], Frank M. Torti[a,b], Suzy V. Torti[b,d,*]

[a]*Department of Cancer Biology, Wake Forest University Health Sciences, Wake Forest University, Winston-Salem, NC, USA*
[b]*Comprehensive Cancer Center, Wake Forest University Health Sciences, Wake Forest University, Winston-Salem, NC, USA*
[c]*Department of Chemistry, University of New Hampshire, Durham, NH, USA*
[d]*Department of Biochemistry, Wake Forest University Health Sciences, Wake Forest University, Winston-Salem, NC, USA*
[e]*Department of Chemistry, Wake Forest University, Winston-Salem, NC, USA*
[f]*Radiation Oncology Branch, National Institutes of Health, Bethesda, MD, USA*

Received 15 October 2003; accepted 23 December 2003

Abstract

Tachpyridine (*N*,*N*′,*N*″-tris(2-pyridylmethyl)-*cis*,*cis*-1,3,5-triaminocyclohexane; tachpyr) is a potent hexadentate iron chelator under preclinical investigation as a potential anti-cancer agent. Tachpyridine induces apoptosis in cultured cancer cells by triggering a mitochondrial pathway of cell death that is p53-independent. To explore the relationship between the chelation chemistry of tachpyridine and its biological activity, a sensitive and specific reversed-phase high-performance liquid chromatography (RP-HPLC) method was devised and used to measure tachpyr and its metal complexes in cells and tissue culture media. Major species identified in cells treated with tachpyr were tachpyr itself, $[Zn(tachpyr)]^{2+}$, and iron coordinated to two partially oxidized species of tachpyridine, $[Fe(tachpyr\text{-}ox\text{-}2)]^{2+}$, and $[Fe(tachpyr\text{-}ox\text{-}4)]^{2+}$. The kinetics of intracellular accumulation of $[Zn(tachpyr)]^{2+}$ and $[Fe(tachpyr\text{-}ox\text{-}2)]^{2+}$ were markedly different: $[Zn(tachpyr)]^{2+}$ rapidly reached plateau levels, whereas intracellular levels of $[Fe(tachpyr\text{-}ox\text{-}2)]^{2+}$ and free tachpyr rose steadily. At the last timepoint measured, 9% of total cellular iron and 13% of total cellular zinc were bound by tachpyridine. Taken together, $[Zn(tachpyr)]^{2+}$, $[Fe(tachpyr\text{-}ox\text{-}2)]^{2+}$, and free tachpyr accounted for virtually all of the tachpyr added, indicating that iron and zinc are the principal metals targeted by tachpyridine in cells. Consistent with these findings, activation of the apoptotic caspases 9 and 3 was blocked in cells pre-treated with either iron or zinc. Pretreatment with either of these metals also completely protected cells from the cytotoxic effects of tachpyridine. These results demonstrate a link between metal depletion and chelator cytotoxicity, and suggest that intracellular chelation of zinc as well as iron may play a role in the cytotoxicity of tachpyridine.

Keywords: Chelator; Zinc; Iron; Caspase; Apoptosis; Chemotherapeutic agent

1. Introduction

Development of iron chelators as therapeutic agents has focused primarily on their use in the treatment of secondary iron overload. However, by binding redox-active iron, chelators may also play a beneficial role in the treatment of pathological conditions mediated by oxidative stress, including ischemia–reperfusion injury, neurodegenerative diseases, and inflammation. In addition, chelators also exhibit toxic propensities that may be deliberately exploited for different purposes: for example, due to their ability to sequester metals essential to tumor growth or to foster redox cycling of bound iron, chelators may be useful as anti-cancer agents [1,2]. Optimizing chelators for these diverse applications will require a precise understanding of their cellular targets.

There has been a growing interest in the use of iron chelators as anti-cancer agents. For example, desferrioxamine, the chelator of choice in the treatment of iron overload, has been utilized both as a single agent and in combination therapy for the treatment of patients with leukemia [3,4] and neuroblastoma [5–9]. However, the relatively modest anti-tumor activity of desferrioxamine has led to an ongoing search for chelators with improved

Abbreviations: SPE, solid phase extraction; PBS, phosphate-buffered saline; IS, internal standard.

* Corresponding author. Tel.: +1-336-716-9357; fax: +1-336-716-0255.
E-mail address: storti@wfubmc.edu (S.V. Torti).

0006-2952/$ – see front matter © 2004 Elsevier Inc. All rights reserved.
doi:10.1016/j.bcp.2003.12.036

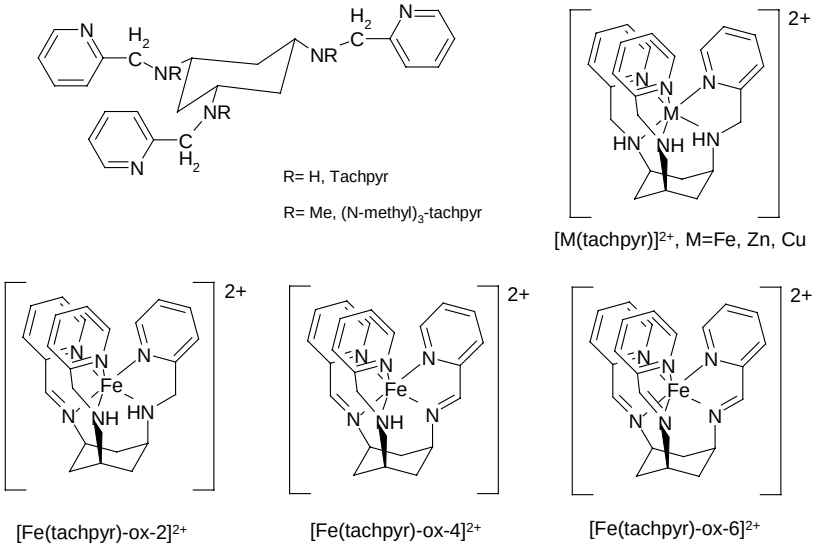

Fig. 1. Molecular structure of tachpyr, (*N*-methyl)$_3$-tachpyr, metal complexes (M = Fe, Zn, Cu) and oxidized species of [Fe(tachpyr-ox-*n*)]$^{2+}$ (*n* = 2, 4, 6).

activity. Tachpyridine represents one chelator under active exploration for its anti-tumor properties. Others include isonicotinoyl hydrazones, thiosemicarbazones, *O*-trensox, as well as microbiological siderophores such as desferrithiocin [1,2].

Tachpyr (*N*,*N*′,*N*″-tris(2-pyridylmethyl)-*cis*,*cis*-1,3,5-triaminocyclohexane) (Fig. 1) is a hexadentate metal chelator based on the framework triamine *cis*,*cis*-1,3,5-triaminocyclohexane. Tachpyr has been shown to chelate divalent metal ions (M = Fe^{2+}, Zn^{2+}, Cu^{2+}, Ca^{2+}, Mg^{2+}, Mn^{2+}) under aqueous or non-aqueous conditions, and the corresponding chelates, $[M(tachpyr)]^{2+}$, have been chemically characterized [10–12]. Tachpyr is toxic to cultured cancer cells, exhibiting an enhanced potency relative to desferrioxamine [13], and activating a caspase cascade that culminates in apoptosis [14]. Further, tachpyr exerts a cytotoxic effect on cells with both mutant and wildtype p53 [15]. Since cancers with mutant p53 represent over 50% of human cancers, and since mutant p53 renders cells resistant to numerous conventional chemotherapeutic agents such as cisplatin and etoposide, this suggests that tachpyr may be of utility in the treatment of tumors that are refractory to treatment with conventional agents. The in vivo anti-tumor properties of the tach family of metal chelators are currently being explored through the Rapid Access to NCI Discovery Resources (RAND) program of the NCI.

The ability to optimally utilize chelators is predicated on a close understanding of the biological basis of their activity. Although some insights have been gained into molecular pathways involved in tachpyr-mediated cell death [14,15], central to an understanding of tachpyr's mode of action is an appreciation of the nature of its metal binding, and the relationship between metal speciation and cytotoxicity. Previous results have shown that the iron, zinc and copper complexes of tachpyr are blocked in their cytotoxic activity, whereas the calcium, magnesium and manganese complexes are not [13]. These results are in accord with the chemistry of tachpyr, and its demonstrated ability to bind with Fe(II), Cu(II) and Zn(II) more strongly than Mn(II), Ca(II) or Mg(II) in aqueous solution [16,17] as well as the propensity of $[Ca(tachpyr)]^{2+}$, $[Mg(tachpyr)]^{2+}$ and $[Mn(tachpyr)]^{2+}$ complexes to dissociate in aqueous media (ref. [10] and Planalp, unpublished observations). Further studies of the chemistry of tachpyr demonstrated that in the presence of equimolar concentrations of iron and zinc, zinc is bound first by tachpyr, followed by iron. However, on prolonged incubation, iron was able to displace zinc [17]. The chemistry of tachpyr is additionally complicated by changes in the ligand that ensue following binding to iron. Thus, in addition to a simple binding reaction, $[Fe(tachpyr)]^{2+}$ readily undergoes iron-mediated oxidative dehydrogenation of its aminomethylene groups to form the monoimino-, diimino- and triimino-complexes (denoted here as $[Fe(tachpyr\text{-}ox\text{-}n)]^{2+}$; *n* = 2, 4, 6) upon exposure to oxygen and/or H_2O_2 (Fig. 1) [12]. The propensity of these species to form in the intracellular environment and their role in the biological activity of tachpyridine has not been assessed.

In order to define the metals that represent important cellular targets of tachpyridine in cells, the extent to which tachpyridine's chemical behavior predicts its cellular activities, and the role of metal chelation in its cytotoxic properties, we developed a quantitative and reproducible method of analysis capable of differentiating among tachpyr and its metal complexes in cells and media. Using this method, we demonstrate that the chemistry of tachpyr accurately predicts its cellular behavior. We demonstrate for the first time that zinc, in addition to iron, is an important cellular target of tachpyr. Further, preincubation of cells with either iron or zinc prior to drug exposure

blocked caspase activation and protected cells from the cytotoxic effects of subsequent challenge with tachpyridine, arguing that metal chelation is an essential component of tachpyridine's cytotoxic action.

2. Materials and methods

2.1. Chemicals and reagents

Tachpyr and (*N*-methyl)$_3$-tachpyr were prepared and their purity confirmed as >99% by ^{1}H and ^{13}C NMR as previously reported [12,16]. HPLC-grade triethylamine (TEA), acetic acid, ammonium hydroxide and Optima-grade acetonitrile, methanol and water were purchased from Fisher Scientific. Citric acid and sodium dodecyl sulfate (SDS; for ion pair chromatography) were from Sigma–Aldrich. All other chemicals were of the highest quality available. Oasis™ HLB 1 ml/10 mg and 3 ml/60 mg extraction cartridges were obtained from Waters. A solid phase extraction vacuum manifold, pre-cut 0.2 μm nylon membrane were purchased from Alltech Associates.

Aqueous standard solutions of $[Fe(tachpyr)]^{2+}$ and $[Fe(tachpyr\text{-}ox\text{-}n)]^{2+}$ ($n = 2, 4, 6$) for validation of HPLC peak assignments were prepared as follows at a concentration of 10^{-3} M and diluted further as needed. A yellow aqueous solution of unoxidized $[Fe(tachpyr)]^{2+}$ (10^{-3} M) was prepared by reaction of equal volumes of tachpyr (0.1 M) and freshly prepared $FeCl_2{\cdot}4H_2O$ (0.1 M) under a nitrogen atmosphere, and then further dilution (1:50). A mixture of $[Fe(tachpyr)]^{2+}$ and $[Fe(tachpyr\text{-}ox\text{-}2)]^{2+}$ (ca. 1:1) was prepared by reaction of d_4-MeOH solutions of $FeCl_3{\cdot}6H_2O$ (0.1 M) and tachpyr (0.1 M) under N_2. The composition was confirmed by ^{1}H NMR spectroscopy. This mixture (total $[Fe] = 0.05$ M) was further diluted (1:50) giving a blue solution.

A set of solutions, $[Fe(tachpyr\text{-}ox\text{-}n)]^{2+}$ ($n = 2, 4, 6$), of increasing degree of oxidation were prepared by addition of 1, 2, and 3 molar equivalents (7.5, 15 and 22 μl, respectively) of $(NH_4)_2S_2O_8$ (0.1 M) to 750 μl samples of the 1:1 $[Fe(tachpyr)]^{2+}$:$[Fe(tachpyr\text{-}ox\text{-}2)]^{2+}$ mixture described above. These solutions exhibited colors of purple, light purple and light purple-brown respectively [12]. UV-Vis spectroscopic studies of the solutions confirmed the formation of the $n = 2, 4, 6$ species, of successively higher n as more oxidizing agent was added. Decreases in signal intensities also indicated that this agent caused partial decomposition of the Fe complexes.

2.2. Cell culture and sample preparation [18]

The human cervical cancer cell line Hela was obtained from ATCC. Cells were cultured in Dulbecco's modified Eagle's medium (DMEM) supplemented with 10% fetal bovine serum, 1% antibiotic mixture (100 units/ml penicillin, 100 μg/ml streptomycin), and maintained at 37 °C in a humidified 5% CO_2 incubator. SUM149 breast cancer cells were a generous gift of Dr. I. Berquin (Wake Forest University Health Sciences). SUM149 cells were grown in serum-free Ham's F12 medium containing 1 mg/ml bovine serum albumin, 5 mM ethanolamine, 10 mM HEPES ([2-hydroxyethyl]piperazine-*N*′-[2-ethanesulfonic acid]), 5 μg/ml transferrin, 10 nM triiodothyronine, 50 nM sodium selenate, 5 μg/ml insulin, 1 μg/ml hydrocortisone, 5 μg/ml gentamycin and 25 μg/ml fungizone in 10% CO_2 as described [19]. Cells were seeded in duplicate 100 mm × 20 mm plastic tissue culture dishes (Falcon, Becton Dickinson) at a density of approximately 2.0×10^7 cells per dish in a volume of 10 ml of media. Approximately 16 h after seeding, media was removed and replaced with fresh media containing tachpyr at a final concentration of 50 μM. Tachpyr metabolites in the growth media were measured following centrifugation of the culture supernate and addition of (*N*-methyl)$_3$-tachpyr to a final concentration of 5 μM as an internal standard (IS) prior to solid phase extraction (SPE). For measurement of tachpyr metabolites in cells, cell monolayers were washed twice with 10 ml of ice-cold phosphate-buffered saline (PBS; pH 7.4) and mechanically detached from the dishes by scraping. Next, cells were suspended in 1 ml of ice-cold PBS (pH 7.4), followed by the addition of 10 μl of IS solution at a final concentration of 10 μM. Total cell number and viability was assessed by trypan blue exclusion in separate dishes treated in parallel to dishes used for HPLC analyses. Under these conditions, viability was 100, 90, and 77% after 4, 8, and 16 h, respectively. Floating cells were collected by centrifugation and added to the cell suspensions to determine total intracellular tachpyr and metabolites. Finally, the cell suspensions were disrupted by two brief (8 s) periods of sonication while the tubes were maintained on ice. The cell lysates were centrifuged at 15,000 rpm, 4 °C for 40 min. The cell lysate supernatant and tissue culture media were immediately subjected to SPE and HPLC as described in the following sections.

2.3. Solid phase extraction procedure [20–22]

Solid phase extraction was performed using a 1 ml/10 mg or 3 ml/60 mg Oasis™ HLB extraction cartridge (Waters) for cell lysates and tissue culture media, respectively. The cartridge was conditioned with 1 ml of methanol and equilibrated with 1 ml of water, then loaded with 1 ml of cell lysate or 10 ml of tissue culture media. After washing with 1 or 2 ml of methanol:NH_4OH:water (5:2:93 v/v/v), the analytes were eluted with 0.2 or 1 ml of acetic acid:methanol (2:98 v/v). In this step, cell lysates and tissue culture media samples were concentrated five- and 10-fold, respectively. No evaporation or reconstitution steps were required. A 25 μl aliquot of final elutes of Hela cell lysates and tissue culture media were analyzed by HPLC.

2.4. HPLC instrumentation

The HPLC system consisted of two Waters 510 pumps, a 717 plus autosampler, and a 490E programmable multi-wavelength detector. Full system control, data acquisition, processing, and reporting were performed using Millennium 3.2 software (Waters). A Sentry™ RP18 guard column (3.9 mm × 20 mm, 5 μm particle size) attached to a Waters SymmetryShield™ RP18 column (4.6 mm × 250 mm, 5 μm particle size) (Waters) was used at ambient temperature with UV-Vis detection at 261 nm, 435 nm and 600 nm. The autosampler temperature was set at 4 °C. The mobile phase was filtered through a 0.2 μm nylon membrane and degassed by sonication prior to use. The flow rate was set at 1.0 ml/min and the injection volume was 25 μl.

2.5. HPLC method development

Tachpyr is a basic, relatively nonpolar compound, while its metal complexes are highly polar and structurally similar to each other. To minimize interactions between basic solutes and silanol groups on the surface of the stationary phase particles, as well as to minimize tailing effects, a Waters SymmetryShield™ RP18 column was selected [23]. A buffering solution of 25 mM citric acid in acetonitrile:water (50:50 v/v) was used as an initial mobile phase. To optimize the separation of the metal species of tachpyr, sodium dodecyl sulfate, an anionic ion-pair reagent, was added to the mobile phase [24–27]. A concentration of 10 mM SDS was found to yield optimal retention times and satisfactory resolution of metal species. In order to simultaneously elute tachpyr metal complexes and the ligand, tachpyr, which has a very different polarity, a gradient elution was used. Based on a series of optimization trials, final mobile phase A contained 10 mM SDS, 25 mM citric acid in acetonitrile:-water (50:50 v/v), and mobile phase B contained 3 mM SDS, 25 mM citric acid and 3 mM triethylamine in acetonitrile:water (50:50 v/v). The optimized elution program consisted of a gradient of 100% A over 17 min followed by 100% B for 28 min, and a return to 100% A over 8 min.

2.6. Selectivity, peak assignment, and interferences

A set of aqueous solutions of $[Zn(tachpyr)]^{2+}$, $[Cu(tachpyr)]^{2+}$, $[Fe(tachpyr)]^{2+}$ and $[Fe(tachpyr\text{-}ox\text{-}n)]^{2+}$ ($n = 2$, 4, 6) reference samples were prepared as described above. These solutions were diluted to 50 μM and injected individually and as a mixture into HPLC. Component peaks were assigned by spiking the mixture with individual substances or substance mixtures. Multi-channel UV-Vis detection was used to further distinguish the peak of $[Fe(tachpyr)]^{2+}$ ($\lambda_{max} = 438$ nm) from $[Fe(tachpyr\text{-}ox\text{-}2)]^{2+}$ ($\lambda_{max} = 435$ and 600 nm) [17].

2.7. Inertness of $[Zn(tachpyr)]^{2+}$, $[Cu(tachpyr)]^{2+}$, and oxidative reactivity of $[Fe(tachpyr\text{-}ox\text{-}n)]^{2+}$ species

Stock solutions of 1 mM tachpyr and (*N*-methyl)$_3$-tachpyr dissolved in methanol or PBS (pH 7.4) can be kept at 4 °C for 3 months. To analyze metal-complex oxidation, metal complex solutions were freshly prepared and kept on ice (0 °C). At 0, 4, 8, 12, 16, 24 and 48 h, Hela cells and tissue culture media were spiked with known concentrations of metal complexes. Solid phase extraction and HPLC analysis were performed. The concentrations at different times were compared to those at 0 h. The results showed that $[Zn(tachpyr)]^{2+}$ and $[Cu(tachpyr)]^{2+}$ complexes remained unchanged for over 48 h, but $[Fe(tachpyr)]^{2+}$ oxidized to $[Fe(tachpyr\text{-}ox\text{-}2)]^{2+}$ completely during the solid phase extraction procedure, and $[Fe(tachpyr\text{-}ox\text{-}2)]^{2+}$ was also gradually oxidized to $[Fe(tachpyr\text{-}ox\text{-}4)]^{2+}$ and $[Fe(tachpyr\text{-}ox\text{-}6)]^{2+}$. Thus, after 4 h, the $[Fe(tachpyr\text{-}ox\text{-}2)]^{2+}$ level was about 97% of its initial level, and was 75% of its initial level after 24 h. Under aerobic conditions, the $[Fe(tachpyr)]^{2+}$ standard sample (50 μM) was entirely oxidized to form $[Fe(tachpyr\text{-}ox\text{-}2)]^{2+}$ and traces of $[Fe(tachpyr\text{-}ox\text{-}4)]^{2+}$ within 5 h. Similarly, after solid phase extraction $[Fe(tachpyr)]^{2+}$ at 5 μM no longer existed in the elution buffer and $[Fe(tachpyr\text{-}ox\text{-}2)]^{2+}$ plus traces of $[Fe(tachpyr\text{-}ox\text{-}4)]^{2+}$ were observed.

These oxidative reactivity studies therefore suggested that rapid sample analysis with quantification of $[Fe(tachpyr\text{-}ox\text{-}2)]^{2+}$ would approximate the combined $[Fe(tachpyr)]^{2+}$ and $[Fe(tachpyr\text{-}ox\text{-}2)]^{2+}$ present in the analyte. Thus, fresh $[Fe(tachpyr)]^{2+}$ standard solutions were prepared prior to each experiment, using degassed methanol or PBS (pH 7.4) as a solvent. The cell and media samples were kept on ice and processed and analyzed as soon as possible, usually within 4 h.

2.8. Validation parameters

Linearity of tachpyr and its metabolites in spiked Hela cells and tissue culture media was investigated at eight concentrations over a range of 0.1–100 and 0.1–25 μM, respectively. Calibration curves were obtained by least-squares linear regression analysis of the peak area ratio of analyte/IS versus analyte concentration. Extraction recovery of tachpyr and its metabolites were determined using solid phase extraction procedures for Hela cells and tissue culture media spiked with known concentrations of tachpyr and its metabolites. The SPE recovery of tachpyr and its metal complex metabolites from Hela cells and tissue culture media was determined by comparing the results ($n = 5$) from SPE and from unextracted pure standards directly injected into the chromatography system. The extraction recovery was from 75.8% for tachpyr to 103.2% for $[Fe(tachpyr)]^{2+}$ complexes. The intra-day repeatability of the method was determined by repeating

Table 1
Validation parameters

Analytes		Hela cells			Tissue culture media		
		[Fe(tachpyr)-ox-2]$^{2+}$	[Zn(tachpyr)]$^{2+}$	Tachpyr	[Fe(tachpyr)-ox-2]$^{2+}$	[Zn(tachpyr)]$^{2+}$	Tachpyr
Linearity ($y = ax + b$)	$a \pm$ S.D.	0.0269 ± 0.0053	0.0237 ± 0.0060	0.0643 ± 0.0005	0.1237 ± 0.0030	0.0488 ± 0.0064	0.2247 ± 0.0023
	$b \pm$ S.D.	−0.0028 ± 0.0185	0.0159 ± 0.0078	−0.0295 ± 0.0102	0.0279 ± 0.0444	0.143 ± 0.1073	−0.5373 ± 0.052
Extraction recovery (%)		103.2	79.6	75.8	95.5	83.6	77.3
R.S.D. (%)		7.2	3.5	8.8	2.1	4.9	5.8
Precision	Intra-day mean (μM)	2.0	2.1	10.7	1.9	2.1	20.5
	R.S.D. (%) ($n = 5$)	6.3	8.9	6.8	2.6	6.8	3.0
	Inter-day mean (μM)	2.0	2.0	10.9	1.9	2.0	20.2
	R.S.D. (%) ($n = 4$ or 5)	4.1	7.4	6.9	6.2	6.7	1.6

Validation parameters for HPLC determination of tachpyr and its metal complexes. Linearity, extraction recovery, intra-day and inter-day precision are shown. The validated concentration for extraction recovery and precision is 2.0 μM for [Fe(tachpyr)-ox-2]$^{2+}$ and [Zn(tachpyr)]$^{2+}$, 10 μM for tachpyr in Hela cells and 20 μM in tissue culture media.

the sample preparation procedure and the analysis of a single sample of Hela cells and tissue culture media spiked with known concentrations of analytes on the same day ($n = 5$). Inter-day reproducibility was assessed by repeating the experiment on 4 or 5 consecutive days. The accuracy (concentration detected × 100/concentration spiked) for tachpyr and its metabolites in cells and media ranged from 100.8 to 108.6 and 97.2 to 104.2%, respectively. The coefficients of variation (CV) for intra-day and inter-day assays for tachpyr and its metabolites in cells and media were less than 9% (see Table 1 for full validation parameters).

2.9. Cytotoxicity assays

Cells were seeded in 96-well plates at 2000 cells per well. Three to six replicate cultures were used. Twenty-four hours later, the medium was replaced with fresh medium containing 25 μM zinc sulfate, 200 μM iron sulfate or no additional supplements (control). (Zinc sulfate was used at lower concentration due to its toxicity at concentrations greater than 25 μM.) After 24 h, metal-containing medium was removed and replaced with basal growth medium. Tachpyridine was added and incubation continued for an additional 72 h. At the end of the 72-h period, viability was measured using an MTS assay [28].

2.10. Caspase assays

Cleavage of caspases was measured by western blotting, as previously described [14].

2.11. Metal measurements

All samples were analyzed in triplicate using a Perkin-Elmer Optima 3100 XL inductively coupled plasma optical emission spectrometer (ICP-OES). The following instrumental parameters were employed throughout: plasma Ar flow, 15 l/min; auxiliary gas flow, 0.5 l/min; nebulizer gas flow rate, 0.8 l/min; power, 1300 W. Standard solutions containing twelve metals dissolved in slightly acidic water spanning the range 0.1–50 μg/ml were used to prepare calibration curves. The averages of the three measurements along with the relative standard deviations were reported for each metal.

3. Results

3.1. Measurement of tachpyridine metal metabolites

Tachpyridine is a hexadentate metal chelator that preferentially binds the biometal ions Fe^{2+}, Zn^{2+}, and Cu^{2+} [2,3]. In addition, chemical analysis has shown that tachpyridine bound to Fe^{2+} undergoes iron-mediated oxidative dehydrogenation to form monoimino-, diimino- and triimino-complexes (designated as [Fe(tachpyr-ox-n)]$^{2+}$; $n = 2$, 4, 6) [12] (Fig. 1). In order to evaluate the contribution of these reactions to the biological activity of tachpyridine, it was first necessary to design an assay to measure the formation of these metabolites in vivo. We therefore devised an HPLC method capable of resolving the structurally similar Fe^{2+}, Zn^{2+}, and Cu^{2+} complexes of tachpyridine as well as the [Fe(tachpyr-ox-n)]$^{2+}$ species. By combining an anionic ion pair reagent with a gradient elution, the separation of these polar species from the relatively nonpolar ligand was achieved in a single step. Fig. 2 illustrates the resolution obtained using this analytic system. The retention times of [Fe(tachpyr-ox-6)]$^{2+}$, [Fe(tachpyr-ox-4)]$^{2+}$, [Fe(tachpyr-ox-2)]$^{2+}$, [Fe(tachpyr)]$^{2+}$, [Zn(tachpyr)]$^{2+}$, [Cu(tachpyr)]$^{2+}$, (*N*-methyl)$_3$-tachpyr and tachpyr were 15.2, 17.0, 18.7, 19.0, 21.0, 22.8, 44.7 and 48.2 min, respectively. The relative standard deviations of retention times varied from 0.9 to 2.1%.

Chromatograms obtained from untreated Hela cells and untreated tissue culture media, along with Hela cells and tissue culture media spiked with 5 μM of [Fe(tachpyr-ox-

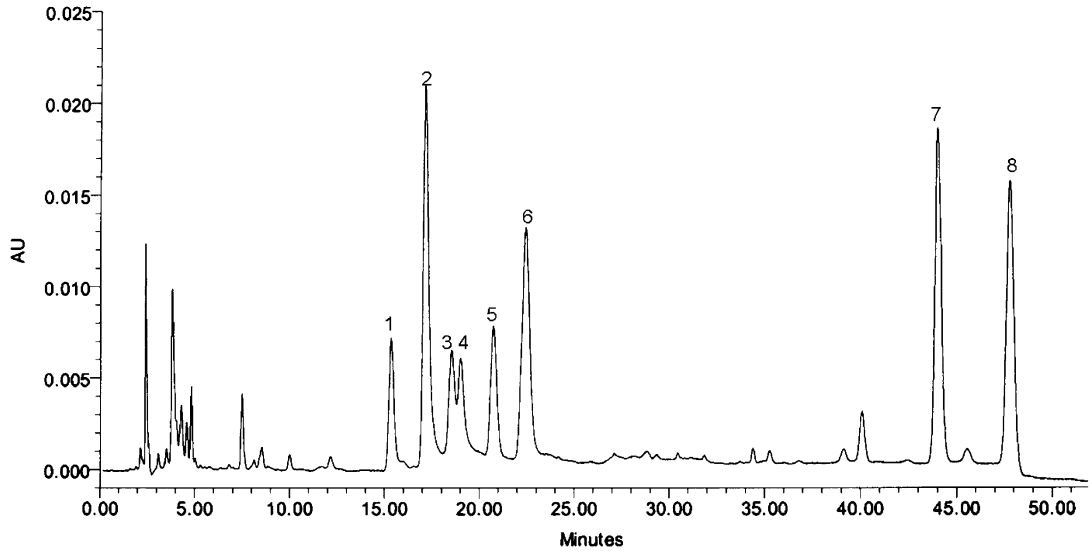

Fig. 2. HPLC separation of tachpyr from its metal complexes. A chromatogram of a mixture of tachpyr and its metal complexes and IS is shown. 1: $[Fe(tachpyr\text{-}ox\text{-}6)]^{2+}$; 2: $[Fe(tachpyr\text{-}ox\text{-}4)]^{2+}$; 3: $[Fe(tachpyr\text{-}ox\text{-}2)]^{2+}$; 4: $[Fe(tachpyr)]^{2+}$; 5: $[Zn(tachpyr)]^{2+}$; 6: $[Cu(tachpyr)]^{2+}$; 7: $(N\text{-methyl})_3$-tachpyr (IS); 8: tachpyr.

$n)]^{2+}$ ($n = 0$, 2, 4, 6), $[Zn(tachpyr)]^{2+}$, $[Cu(tachpyr)]^{2+}$, tachpyr and 50 μM of the internal standard $(N\text{-methyl})_3$-tachpyr are shown in Fig. 3. No interference peaks were found at the retention times of these standards. The media and cells spiked with $(N\text{-methyl})_3$-tachpyr were incubated for 2 h followed by HPLC analysis. No chelation was observed under these conditions (data not shown), indicating that $(N\text{-methyl})_3$-tachpyr could be used as a stable internal standard, and that it did not interfere with the reactions of tachpyr.

HPLC method validation was performed by assessing linearity, extraction recovery, intra-day and inter-day precision. Linear ranges were 0.5–100 μM for tachpyr and 0.25–25 μM for metabolites, with correlation coefficients ranging from 0.9904 to 1. The limit of detection (LOD; defined as the lowest concentration that produces a response two times the noise level) was 0.1 μM for metal complexes and 0.25 μM for tachpyr, and the limit of quantification (LOQ; defined as the lowest concentration that can be accurately measured, producing a signal to noise ratio of 5) was 0.25 μM for metal complexes and 0.5 μM for tachpyr. Validation parameters are shown in Table 1.

3.2. Identification of intra- and extracellular metal metabolites following treatment of cells with tachpyridine

Using this analytic method, we assessed the formation of metal metabolites in cells treated with tachpyridine. Hela

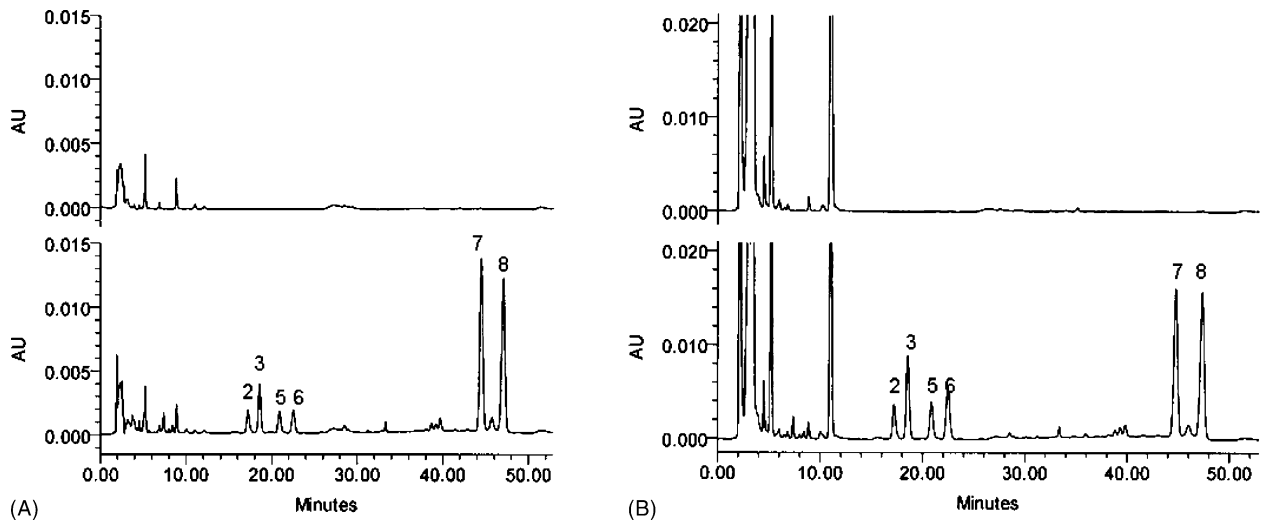

Fig. 3. Components of cell extracts and tissue culture media do not interfere with HPLC separation of tachpyr from its metal complexes. Shown are chromatograms of untreated lysates and media either unspiked (upper panels) or spiked (lower panels) with 5 μM each of $[Fe(tachpyr\text{-}ox\text{-}4)]^{2+}$, $[Fe(tachpyr\text{-}ox\text{-}2)]^{2+}$, $[Zn(tachpyr)]^{2+}$, $[Cu(tachpyr)]^{2+}$ and 50 μM of tachpyr and internal standard (A) Hela cell lysate, (B) tissue culture media. 2: $[Fe(tachpyr\text{-}ox\text{-}4)]^{2+}$; 3: $[Fe(tachpyr\text{-}ox\text{-}2)]^{2+}$; 5: $[Zn(tachpyr)]^{2+}$; 6: $[Cu(tachpyr)]^{2+}$; 7: $(N\text{-methyl})_3$-tachpyr (IS); 8: tachpyr.

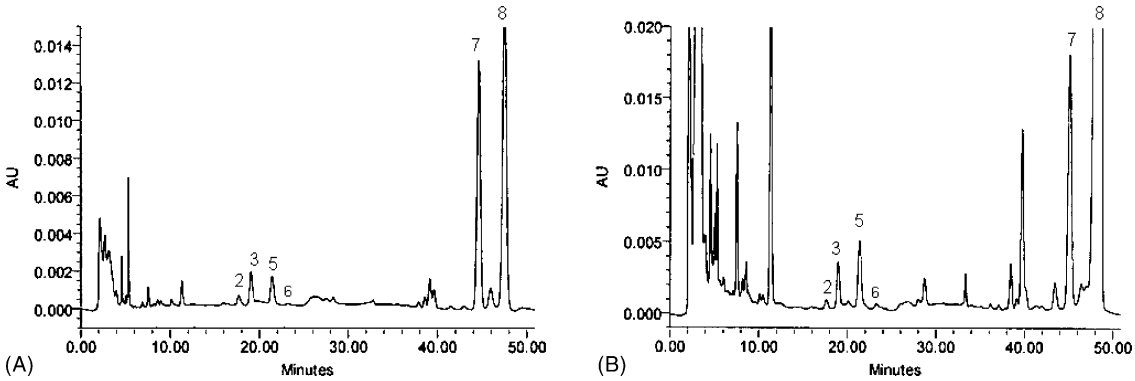

Fig. 4. Isolation of tachpyr and its metal complexes from Hela cells and media. Shown is a chromatogram of (A) Hela cells and (B) DMEM media 16 h after treatment with 50 μM tachpyr. 2: $[Fe(tachpyr\text{-}ox\text{-}4)]^{2+}$; 3: $[Fe(tachpyr\text{-}ox\text{-}2)]^{2+}$; 5: $[Zn(tachpyr)]^{2+}$; 6: $[Cu(tachpyr)]^{2+}$; 7: (N-methyl)$_3$-tachpyr (IS); 8: tachpyr.

cells were treated with 50 μM tachpyr for 16 h, and cells and tissue culture media were collected and analyzed by HPLC. As shown in Fig. 4, major species detected were tachpyr itself, $Zn(tachpyr)^{2+}$, $[Fe(tachpyr\text{-}ox\text{-}2)]^{2+}$, and $[Fe(tachpyr\text{-}ox\text{-}4)]^{2+}$. As discussed in Section 2, due to oxidation that occurs during the analytic procedure, the $[Fe(tachpyr\text{-}ox\text{-}2)]^{2+}$ peak is best considered as the sum of $[Fe(tachpyr)]^{2+}$ and $[Fe(tachpyr\text{-}ox\text{-}2)]^{2+}$. Occasionally, small quantities of $[Fe(tachpyr\text{-}ox\text{-}4)]^{2+}$ were observed, which could indicate slight oxidation of $[Fe(tachpyr\text{-}ox\text{-}2)]^{2+}$ during the analysis, or the intracellular formation of $[Fe(tachpyr\text{-}ox\text{-}4)]^{2+}$. The $[Fe(tachpyr\text{-}ox\text{-}6)]^{2+}$ complex was not observed.

3.3. Kinetics and quantification of metabolite formation in cells

Fig. 5 shows the average quantity of metal complexes in Hela cells and tissue culture media for three independent experiments in which cells were treated in duplicate with 50 μM tachpyr over a time course of 16 h. In Hela cells, $[Zn(tachpyr)]^{2+}$ increased quickly to a peak level of 0.23 nmol/10^6 cells ($t_{max} = 1$ h) and rapidly fell to a plateau level of 0.16 nmol/10^6 cells and a final concentration of 0.17 nmol/10^6 cells (16 h), while $[Fe(tachpyr\text{-}ox\text{-}2)]^{2+}$ gradually rose to a final concentration of 0.08 nmol/10^6 cells. The increase in cellular tachpyr level and decrease in tachpyr level of tissue culture media indicate gradual cellular uptake of tachpyr and increasing metal chelation by tachpyr. Thus the concentration of tachpyr in tissue culture media decreased as the total amount of $[M(tachpyr)]^{2+}$ in tissue culture media increased and the tachpyr level in Hela cells increased to 0.60 nmol/10^6 cells ($t_{max} = 16$ h). Simultaneously, the tissue culture media concentrations of $[Zn(tachpyr)]^{2+}$ and $[Fe(tachpyr\text{-}ox\text{-}2)]^{2+}$ reached final values of 4.65 and 1.71 μM, respectively (16 h). $[Cu(tachpyr)]^{2+}$ was generally below the limit of quantification both in Hela cells and tissue culture media (ca. $\leq$0.01 nmol/10^6 cells). The total recovery of tachpyr in Hela cells and tissue culture media ranged from 93 to 103% of the total amount of tachpyr added.

In order to test the fraction of intracellular iron and zinc that could be accessed by tachpyridine, total iron and zinc content were measured in untreated Hela cells by atomic absorption. Total iron content was 0.91 ± 0.32 nmol/10^6 cells, zinc content was 1.22 ± 0.6 nmol/10^6 cells, and copper content was 0.03 ± 0.01 nmol/10^6 cells (mean $\pm$ S.D., $n = 4$). Thus, in cells treated for 16 h, approximately 9% of total cellular iron and 13% of total cellular zinc are bound to tachpyridine.

To determine whether this general pattern of accumulation differed among cell types, the accumulation of tachpyridine and its metal metabolites was also assessed in SUM149 cells, a breast epithelial cell line. As shown in Fig. 6, an overall similarity in the pattern of uptake was seen. In both cell types, $[Zn(tachpyr)]^{2+}$ complexes formed initially, followed by the gradual accumulation of $[Fe(tachpyr\text{-}ox\text{-}2)]^{2+}$ complexes. After 16 h, the mean ratio of Fe/Zn complexes ranged from 0.4 to 1.1 in the two cell types, and the ratio of total intracellular metal complexes ($[Fe(tachpyr\text{-}ox\text{-}2)]^{2+}$ plus $[Zn(tachpyr)]^{2+}$) to free ligand ranged from 0.4 to 0.6. These values were not statistically different between the two cell types ($P > 0.2$, Student's t-test).

3.4. Metal protection from the cytotoxic effect of tachpyridine

These results suggested that zinc as well as iron might be important cellular targets of tachpyridine, and that chelation of both metals might play a role in the cytotoxicity of this chelator. To test this prediction, SUM149 cells were preincubated with either zinc or iron in growth media for 24 h. Excess metal was then removed, and cells treated with tachpyridine for 72 h. As shown in Fig. 7, pretreatment with either iron or zinc was able to protect cells from the cytotoxic effect of tachpyridine.

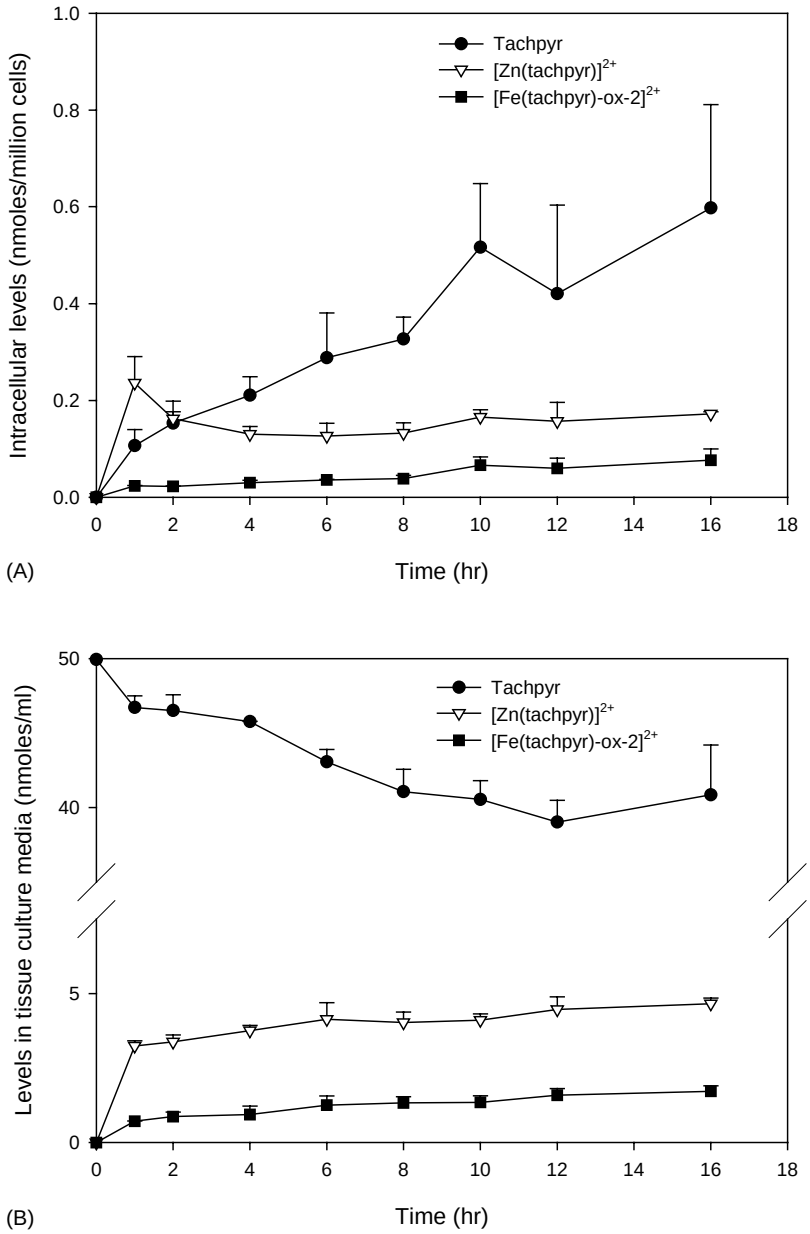

Fig. 5. Time course of accumulation of tachpyr and its metal complexes in Hela cells. Means and standard deviations (error bars) of $[Zn(tachpyr)]^{2+}$, $[Fe(tachpyr\text{-}ox\text{-}2)]^{2+}$ and tachpyr in 50 μM tachpyr treated (A) Hela cells, (B) tissue culture media ($n = 3$).

3.5. Metal pretreatment prevents caspase activation

Caspases are proteolytic enzymes that play critical roles in the initiation and execution of apoptosis. Previous results have shown that tachpyridine triggers a mitochondrial pathway of apoptosis characterized by the early activation of caspase 9 followed by activation of caspase 3 [14]. To test whether metal pretreatment could inhibit caspase activation, cells were pretreated for 24 h with media containing either excess iron or zinc. Cells were then washed and treated with tachpyridine in normal growth medium. In agreement with previous results [14], treatment with tachpyridine triggered the activation of caspases 9 and 3, as measured by the appearance of the cleaved (active) forms of these proteases (Fig. 8). As shown in Fig. 8, pretreatment with iron or zinc completely blocked cleavage of both the intitiator caspase 9 as well as the executioner caspase 3.

4. Discussion

Although the distribution of biometals complexed by synthetic chelating agents is of great importance to their biological effects, there are relatively few reports of attempts to identify intra- and extracellular metal complexes resulting from chelator treatment [29,30]. To our knowledge, complexes of tachpyr have not been previously studied.

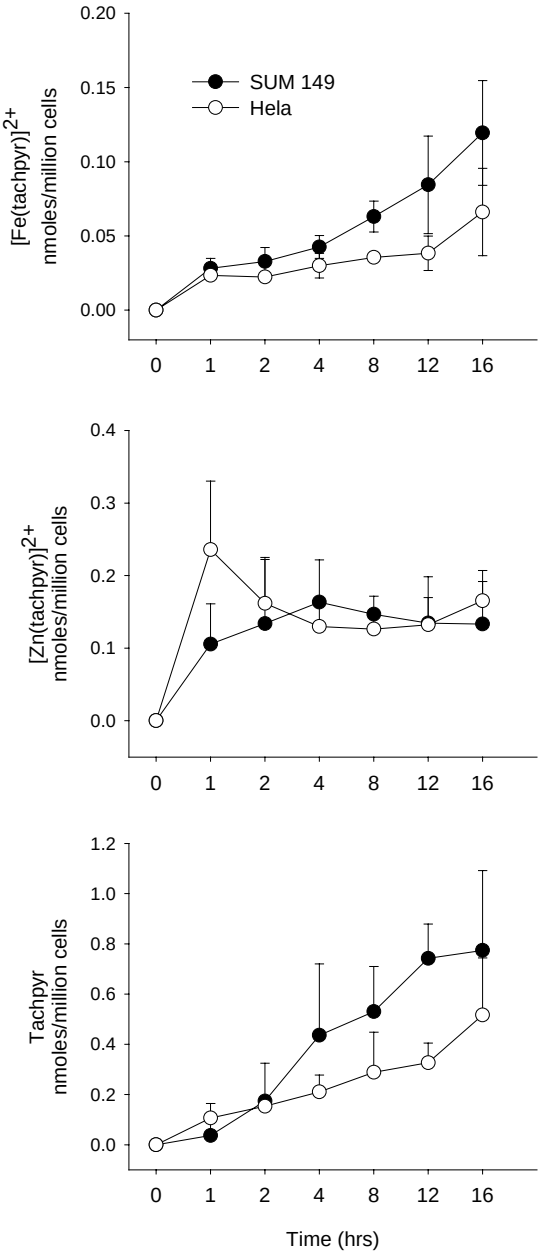

Fig. 6. Tachpyr and its metal metabolites accumulate intracellularly with similar kinetics in two different cell types. SUM149 or Hela cells were exposed to 50 μM tachpyridine for the indicated lengths of time and intracellular concentrations of $[Zn(tachpyr)]^{2+}$, $[Fe(tachpyr)]^{2+}$ and free tachpyr measured by HPLC. Shown are the means and standard deviations of three independent experiments.

Using an analytic method that simultaneously quantifies both tachpyr and its metal complexes, we measured the rate of accumulation of the free ligand and its metal complexes in cells treated with tachpyridine. We observed that in aggregate, the summed concentrations of $[Zn(tachpyr)]^{2+}$, $[Fe(tachpyr\text{-}ox\text{-}2)]^{2+}$, $[Cu(tachpyr)]^{2+}$ and free tachpyr account for virtually all of the tachpyr added. Thus, although tachpyr complexes with Mg^{2+}, Ca^{2+}, and Mn^{2+} can be formed in nonaqueous solvent [13], results presented here suggest that these complexes are labile in vivo. Zinc and iron complexes of tachpyridine were the predominant species identified (Fig. 4). Although tachpyr has a good affinity for Cu^{2+} [31], this complex was present in very small quantities in our analysis. This likely reflects the low overall levels of copper in the cell, which are less than one-tenth the levels of zinc or iron (see Section 3), and which approach the limits of detection of our analysis [32]. The low levels of copper complexes we detect may also reflect the relative inaccessibility of copper coordinated to cellular ligands. Thus, while intracellular iron and zinc may readily be detected, e.g. by fluorescent sensors [33–35], this is not the case for copper. Nevertheless, copper chelation may represent a quantitatively small but qualitatively important mode of action of tachpyridine. Together, zinc, iron and copper represent the primary cellular metals targeted by tachpyridine.

Chemical analysis has demonstrated that upon binding of iron, tachpyr undergoes iron-mediated oxidative dehydrogenation, leading to the formation of monoimino-, diimino-, triimino-complexes $[Fe(tachpyr\text{-}ox\text{-}n)]^{2+}$ ($n = 2, 4, 6$) [12]. Furthermore, tachpyr binds Fe(III) reductively to a mixture of $[Fe(tachpyr)]^{2+}$ and $[Fe(tachpyr\text{-}ox\text{-}2)]^{2+}$ [Planalp, unpublished observations]. Due to the propensity of $[Fe(tachpyr)]^{2+}$ to oxidize to $[Fe(tachpyr\text{-}ox\text{-}2)]^{2+}$ during the course of the analysis, we were unable to determine which of these two species predominates in vivo. Nevertheless, our experiments clearly indicate that in combination, these two species represent the predominant species of iron complexes in cells, and that further oxidation states ($[Fe(tachpyr\text{-}ox\text{-}4)]^{2+}$ and $[Fe(tachpyr\text{-}ox\text{-}6)]^{2+}$) are rarely detected. This may be due to a slow rate of formation of these species in the intracellular environment, or to their more rapid decomposition, since a probe of oxidation with $S_2O_8^{2-}$ indicated a greater tendency to decomposition as oxidation progressed (R. Planalp, unpublished observations).

The kinetics of the accumulation of zinc and iron complexes of tachpyr were markedly different. There was a reproducible trend in which tachpyr and $[Fe(tachpyr)]^{2+}$ complexes accumulated steadily, while $[Zn(tachpyr)]^{2+}$ reached its maximal concentration much more rapidly (Fig. 6). Although little inter-experiment variability in absolute concentrations was seen in earlier timepoints, variability increased at later times. This may in part be attributable to the variation in rate of cell kill by tachpyr, since R.S.D. was greatest at the 12 and 16 h timepoints, when the fraction of cells undergoing cell death began to increase. Measurements of total iron and zinc in Hela cells by atomic absorption indicated that by 16 h, tachpyridine bound approximately 9% of the total iron and 13% of the total zinc in cells. This is comparable to estimates of the fraction of intracellular zinc that reside in labile pools [36]. In the case of iron, this value is at or above values typically assigned to the size of the labile iron pool [37], suggesting that tachpyr may be able to access iron from intracellular sites in addition to the labile pool, or that it may act as an intracellular sink that intercepts and

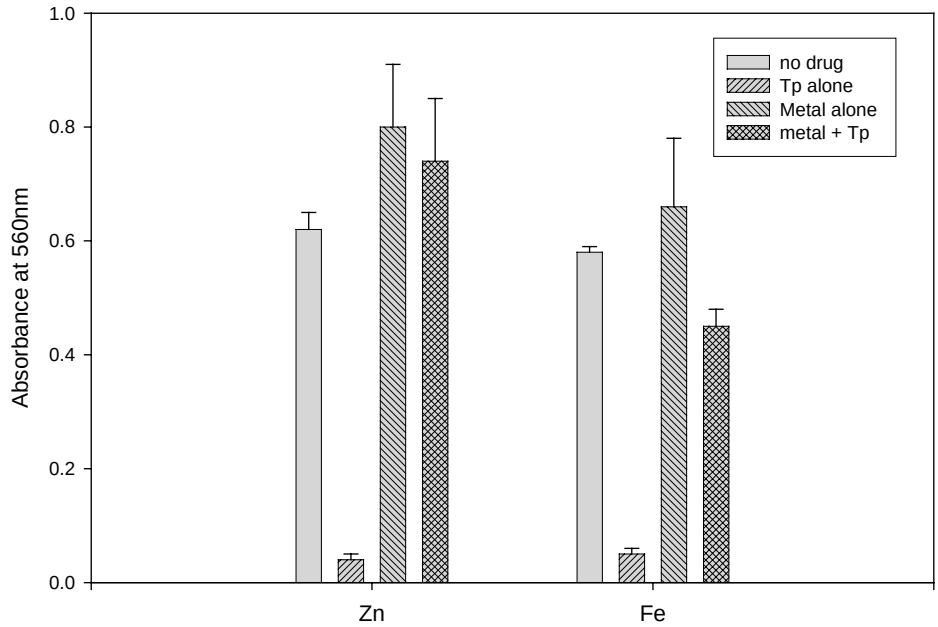

Fig. 7. Protection from tachpyridine cytotoxicity by pre-treatment with zinc or iron. SUM149 cells were treated for 24 h with growth medium containing no additional metals, 25 μM zinc sulfate or 200 μM iron sulfate. After 24 h cells were washed, the medium replaced with medium containing no supplements, and 16 μM tachpyridine added. Incubation was continued for 72 h and viable cells assessed by an MTS assay. Means and standard deviations of three replicate cultures are shown. A representative experiment of three independent experiments is shown.

captures iron as it cycles through the labile pool. In any case, our results indicate that tachpyridine is highly effective in accessing both cellular iron and zinc. The ability to effectively capture the preponderance of intracellularly available zinc and iron may contribute to the potent pro-apoptotic effect of tachpyridine.

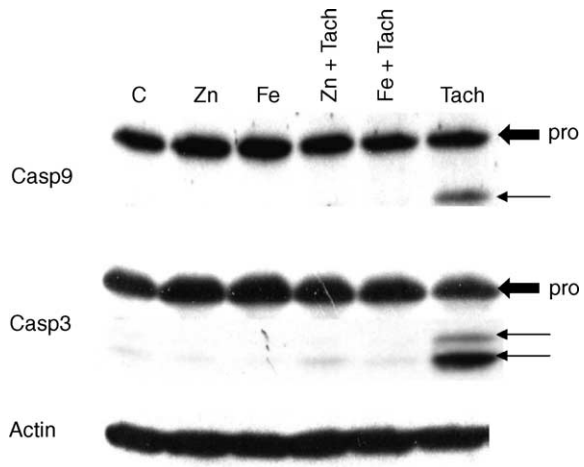

Fig. 8. Metal pretreatment prevents caspase activation. SUM149 cells were pretreated for 24 h with growth medium containing no additional metals, 25 μM zinc sulfate or 200 μM iron sulfate. After 24 h cells were washed, and the medium replaced with medium containing no additional metals and 16 μM tachpyridine. Controls were treated identically, except that tachpyridine was omitted. Cells were harvested 32 h after the addition of tachpyridine and lysates prepared and analyzed for caspase cleavage by western blotting. Lanes represent cells treated with control medium throughout (C); cells pretreated with zinc-supplemented medium, followed by control medium (Zn); cells pretreated with iron-supplemented medium, followed by control medium (Fe); cells pretreated with zinc-supplemented medium, followed by tachpyridine (Zn + Tach); cells pretreated with iron-supplemented medium, followed by tachpyridine (Fe + Tach); cells pretreated with control medium, followed by tachpyridine (tach). Arrows denote the precursor (pro) and cleaved forms of caspases 9 and 3. β-Actin was used as a loading control.

The time course of intracellular metal speciation of tachpyr in Hela cells was remarkably concordant with the coordination chemistry of tachpyr in aqueous pH 7.4 media. In a study of the coordination preference of tachpyr, one molar equivalent of tachpyr was reacted with a mixture of one equivalent of zinc (as Zn(II)(aq)) and one of iron (as an Fe(II)/Fe(III) mixture) in aerobic aqueous pH 7.4 solvent [17]. Tachpyr strongly favored Zn(II) initially ($90 \pm 10\%$ after 5 min), but of a period of 48 h the proportion of $[Zn(tachpyr)]^{2+}$ dropped to $56 \pm 10\%$ while that of $[Fe(tachpyr\text{-}ox\text{-}n)]^{2+}$ ($n = 2, 4$) grew. Similarly, the results presented here demonstrate that after 1 h, the proportion of Zn(tachpyr) to Fe(tachpyr) complexes in Hela cells was $90 \pm 3\%$, whereas after 16 h it had dropped to $70 \pm 11\%$. A similar overall pattern of metal complex formation and ligand accumulation was seen in two different cell types (Fig. 6), although in SUM149 cells the decline in zinc complexes over time was not seen.

The ability of tachpyridine to access intracellular pools of both iron and zinc led us to test whether it might be possible to protect cells from the cytotoxic effects of tachpyridine by preloading cells with these metals. As shown in Fig. 7, pretreatment with iron or zinc did indeed effectively protect cells from tachpyridine cytotoxicity. Since tachpyridine exerts its apoptotic effect by activating caspases, proteolytic enzymes that play a key role in executing the death pathway in cells, we assessed the effect of metal pretreatment on caspase activation. As shown in Fig. 8, pretreatment with iron or zinc was able

to prevent activation of caspases 9 and 3 in cells treated with tachpyridine. This suggests that zinc and iron may inhibit cell death triggered by tachpyridine by preventing the activation of caspases, either by direct or indirect mechanisms. For example, key iron-dependent enzymes include ribonucelotide reductase, mitochondrial electron transport proteins, hydroxylating enzymes, lipoxygenases, cyclooxygenases, as well as cytosolic aconitase/IRP-1 [38]. If tachpyridine initiates apoptosis by accessing metals bound to these or other critical cellular enzymes, preloading cells with iron or zinc may provide sufficient ''decoy'' targets for tachpyridine to protect these critical cellular proteins. Alternatively or additionally, pretreatment with metals may induce cytoprotective pathways that reduce susceptibility to apoptosis. For example, zinc may directly inhibit the proteolytic activity of caspases, particularly caspase 3 [39–41].

Careful assessment of intracellular metal speciation may be generally useful in providing insights into the mode of action of iron chelators, since iron chelators are not completely selective in their metal binding activity, despite substantial preference for iron over other metals. For example in the case of tachpyr, preliminary studies [17] and comparison with model compounds indicate a lower limit of 10^2 and upper limit of 10^7 for the ratio $K_f([Fe(tachpyr)]^{2+})/K_f([Zn(tachpyr)]^{2+})$. Despite this considerable thermodynamic preference for iron, the experiments presented here demonstrate an important ability of zinc as well as iron to modulate the apoptotic effect of tachpyridine. Even more remarkably, desferrioxamine, a chelator in widespread clinical use for the treatment of iron overload, has a formation constant for iron that exceeds that of its formation constant for zinc by over 20 orders of magnitude [42]. Deferiprone, another clinically used iron chelator, exhibits a similar substantial preference for Fe^{3+} over Zn^{2+}, with formation constants of 10^{37} for Fe^{3+} and 10^{13} for Zn^{2+} [43]. Nevertheless, treatment of thymocytes with either desferrioxamine or deferiprone led to a rapid depletion of intracellular zinc, an effect that was also observed following administration of deferiprone to mice [44]. Further, apoptosis induced by deferiprone was prevented by treatment with zinc both in vitro and in vivo. Such discordances between thermodynamic binding preferences and in vivo effects of chelators underscore the value of direct measurements of metal complex formation, such as reported here. Further, they suggest that interaction with zinc may be a generally important but understudied determinant of the biological effects of iron chelators.

Collectively, our experiments demonstrate that tachpyridine chelates both iron and zinc in cells, and point to a role for zinc as well as iron depletion in the cytotoxic activity of tachpyridine. Compounds that act as chelators may have effects in addition to metal depletion (for example, iron complexes of tachpyridine [45] as well as other chelators [43], may generate free radicals). Although cells treated with tachpyridine exhibit characteristics of iron depletion, such as ferritin repression [13], a relationship between metal depletion and apoptosis has not been directly shown. Here, we demonstrate that repletion with iron or zinc can prevent cell death induced by tachpyridine, providing a link between metal depletion and tachpyridine-induced cell death. The identification of critical iron and zinc-dependent enzymes targeted by intracellular metal chelators, coupled with studies directed at elucidating how disruption of their function leads to apoptosis, may yield important insights into how the activity of metal chelators may be controlled.

Acknowledgments

This work was supported in part by grant DK 57781 from the National Institutes of Health (SVT). We are grateful to Joan L. Buss for thoughtful suggestions and critical reading of the manuscript. We thank members of the National Cancer Institute Rapid Access to Intervention Development (RAID) and National Cancer Institute Rapid Access to NCI Discovery Resources (RAND) Programs for preclinical studies and for helpful advice and insights.

References

[1] Le N, Richardson D. The role of iron in cell cycle progression and the proliferation of neoplastic cells. Biochim Biophys Acta 2002;1603: 31–46.
[2] Buss JL, Torti FM, Torti SV. The role of iron chelation in cancer therapy. Curr Med Chem 2003;10:1021–34.
[3] Estrov Z, Tawa A, Wang XH, Dube ID, Sulh H, Cohen A, et al. In vitro and in vivo effects of deferoxamine in neonatal acute leukemia. Blood 1987;69:757–61.
[4] Dezza L, Cazzola M, Danova M, Carlo-Stella C, Bergamaschi G, Brugnatelli S, et al. Effects of desferrioxamine on normal and leukemic human hematopoietic cell growth: in vitro and in vivo studies. Leukemia 1989;3:104–7.
[5] Donfrancesco A, Deb G, Dominici C, Pileggi D, Castello MA, Helson L. Effects of a single course of deferoxamine in neuroblastoma patients. Cancer Res 1990;50:4929–30.
[6] Frantz CN, Bernstein M, Castleberry R, Vietti T. Proc Am Soc Clin Oncol 1994;13:416.
[7] Blatt J. Deferoxamine in children with recurrent neuroblastoma. Anticancer Res 1994;14:2109–12.
[8] Donfrancesco A, De Bernardi B, Carli M, Mancini A, Nigro M, De Sio L, et al. Deferoxamine followed by cyclophosphamide, etoposide, carboplatin, thiotepa, induction regimen in advanced neuroblastoma: preliminary results. Italian Neuroblastoma Cooperative Group. Eur J Cancer 1995;31:612–5.
[9] Donfrancesco A, Deb G, Angioni A, Maurizio C, Cozza R, Jenkner A, et al. D-CECaT: a breakthrough for patients with neuroblastoma. Anticancer Drugs 1993;4:317–21.
[10] Park G, Przyborowska A, Ye N, Tsoupas N, Bauer C, Broker G, et al. Steric effects caused by *N*-alkylation of the tripodal chelator *N*,*N*′,*N*″-tris(2-pyridylmethyl)-*cis*,*cis*-1,3,5-triaminocyclohexane (tachpyr): structural and electronic properties of the Mn(II), Co(II), Ni(II), Cu(II) and Zn(II) complexes. J Chem Soc, Dalton Trans 2003;318.
[11] Planalp RP, Lai S, Lu G, Przyborowska AM, Park G, Rogers RD, et al. Biometals 2002: 3rd International Biometals Symposium, London, UK, April 2002, p. E4.

[12] Park G, Lu F, Ye N, Brechbiel M, Torti S, Torti F, et al. Novel iron complexes and chelators based on *cis*,*cis*-1,3,5-triaminocyclohexane: iron-mediated ligand oxidation and biochemical properties. J Biol Inorg Chem 1998;3:449–57.
[13] Torti SV, Torti FM, Whitman SP, Brechbiel MW, Park G, Planalp RP. Tumor cell cytotoxicity of a novel metal chelator. Blood 1998;92: 1384–9.
[14] Greene BT, Thorburn J, Willingham MC, Thorburn A, Planalp RP, Brechbiel MW, et al. Activation of caspase pathways during iron chelator-mediated apoptosis. J Biol Chem 2002;277:25568–75.
[15] Abeysinghe RD, Greene BT, Haynes R, Willingham MC, Turner J, Planalp RP, et al. p53-independent apoptosis mediated by tachpyridine, an anti-cancer iron chelator. Carcinogenesis 2001;22:1607–14.
[16] Bowen T, Planalp RP, Brechbiel MW. An improved synthesis of *cis*,*cis*-1,3,5-triaminocyclohexane. Synthesis of novel hexadentate ligand derivatives for the preparation of gallium radiopharmaceuticals. Bioorg Med Chem Lett 1996;6:807.
[17] Planalp RP, Przyborowska AM, Park G, Ye N, Lu FH, Rogers RD, et al. Novel cytotoxic chelators that bind iron(II) selectively over zinc(II) under aqueous aerobic conditions. Biochem Soc Trans 2002; 30:758–62.
[18] Boyd G, Smyth JF, Jodrell DI, Cummings J. High-performance liquid chromatographic technique for the simultaneous determination of lactone and hydroxy acid forms of camptothecin and SN-38 in tissue culture media and cancer cells. Anal Biochem 2001;297:15–24.
[19] Berquin IM, Dziubinski ML, Nolan GP, Ethier SP. A functional screen for genes inducing epidermal growth factor autonomy of human mammary epithelial cells confirms the role of amphiregulin. Oncogene 2001;20:4019–28.
[20] Cheng YF, Neue UD, Bean L. Straightforward solid-phase extraction method for the determination of verapamil and its metabolite in plasma in a 96-well extraction plate. J Chromatogr A 1998;828: 273–81.
[21] Cheng YF, Neue UD, Woods LL. Novel high-performance liquid chromatographic and solid-phase extraction methods for quantitating methadone and its metabolite in spiked human urine. J Chromatogr B: Biomed Sci Appl 1999;729:19–31.
[22] Rouan MC, Marfil F, Mangoni P, Séchaud R, Humbert H, Maurer G. Determination of a new oral iron chelator, ICL670, and its iron complex in plasma by high-performance liquid chromatography and ultraviolet detection. J Chromatogr B 2001;755:203–13.
[23] Technical reports. Comparison guide to C18 reversed phase HPLC columns. MAC-MOD Analytical, Inc.
[24] Sarzanini C. High-performance liquid chromatography: trace metal determination and speciation. Adv Chromatogr 2001;41:249–310.
[25] Tomlinson E, Jefferies TM, Riley CM. Ion-pair high-performance liquid chromatography. J Chromatogr 1978;159:315–58.
[26] Hart SJ, Tontodonati R, Calder IC. Reversed-phase chromatography of urinary metabolites of paracetamol using ion suppression and ion pairing. J Chromatogr 1981;225:387–405.
[27] Liang H, Kays MB, Sowinski KM. Separation of levofloxacin, ciprofloxacin, gatifloxacin, moxifloxacin, trovafloxacin and cinoxacin by high-performance liquid chromatography: application to levofloxacin determination in human plasma. J Chromatogr B 2002;772: 53–63.
[28] Cory AH, Owen TC, Barltrop JA, Cory JG. Use of an aqueous soluble tetrazolium/formazan assay for cell growth assays in culture. Cancer Commun 1991;3:207–12.
[29] Epemolu R, Ackerman R, Porter J, Hider R, Damani L, Singh S. HPLC determination of 1,2-diethyl-3-hydroxypyridin-4-one (CP94), its iron complex [Fe(III) (CP94)3] and glucuronide conjugate [CP94-GLUC] in serum and urine of thalassaemic patients. J Pharm Biomed Anal 1994;12:923–30.
[30] Wang P, Lee HK. Recent applications of high-performance liquid chromatography to the analysis of metal complexes. J Chromatog A 1997;789:437–51.
[31] Ma D, Lu F, Overstreet T, Milenic DE, Brechbiel MW. Novel chelating agents for potential clinical applications of copper. Nucl Med Biol 2002;29:91–105.
[32] Gulumian M, Hancock RD, Rollin HB. Different fractions of metal ions in biological fluids and their physiological roles. Handbook Metal–Ligand Interact Biol Fluids: Bioinorg Chem 1995;1:93–107.
[33] Burdette SC, Walkup GK, Spingler B, Tsien RY, Lippard SJ. Fluorescent sensors for Zn(2+) based on a fluorescein platform: synthesis, properties and intracellular distribution. J Am Chem Soc 2001;123: 7831–41.
[34] Hirano T, Kikuchi K, Urano Y, Nagano T. Improvement and biological applications of fluorescent probes for zinc, ZnAFs. J Am Chem Soc 2001;124:6555–62.
[35] Petrat F, De Groot H, Sustmann R, Rauen U. The chelatable iron pool in living cells: a methodically defined quantity. Biol Chem 2002;383: 489–502.
[36] Tamura T, Sadakata N, Oda T, Maramatsu T. Role of zinc ions in ricin-induced apoptosis in U937 cells. Toxicol Lett 2002;132:141–51.
[37] Breuer W, Epsztejn S, Cabantchik ZI. Iron acquired from transferrin by K562 cells is delivered into a cytoplasmic pool of chelatable iron(II). J Biol Chem 1995;270:24209–242115.
[38] Minotti G, Recalcati S, Mordente A, Liberi G, Calafiore A, Mancuso C, et al. The secondary alcohol metabolite of doxorubicin irreversibly inactivates aconitase/iron regulatory protein-1 in cytosolic fractions from human myoxardium. FASEB J 1998;12:541–52.
[39] Perry DK, Smyth MJ, Stennicke HR, Salvesen GS, Duriez P, Poirier GG, et al. Zinc is a potent inhibitor of the apoptotic protease, caspase-3. A novel target for zinc in the inhibition of apoptosis. J Biol Chem 1997;272:18530–3.
[40] Chimienti F, Seve M, Richard S, Mathieu J, Favier A. Role of cellular zinc in programmed cell death: temporal relationship between zinc depletion, activation of caspases, and cleavage of Sp family transcription factors. Biochem Pharmacol 2001;62:51–62.
[41] Stennicke HR, Salveson GS. Biochemical characteristics of caspases-3, -6, -7, and -8. J Biol Chem 1997;272:25719–23.
[42] Martell AE, Smith RM. Critical stability constants. New York: Plenum Press; 1974–1989.
[43] Liu ZD, Hider RC. Design of clinically useful iron(III)-selective chelators. Med Res Rev 2002;22:26–64.
[44] MacLean KH, Cleveland JL, Porter JB. Cellular zinc content is a major determinant of iron chelator-induced apoptosis of thymocytes. Blood 2001;98:3831–9.
[45] Samuni AM, Krishna MD, DeGraff W, Russo A, Planalp RP, Brechbiel M, et al. Mechanisms underlying the cytotoxic effects of Tachpyr—a novel metal chelator. Biochim Biophys Acta 2002;1571:211–8.